

## DEVELOPMENT OF A GAS SENSOR FOR GREEN LEAF VOLATILE DETECTION

*Shakir-ul Haque Khan<sup>1</sup>, Sayali Tope<sup>1</sup>, Rana Dalpati<sup>2</sup>, Kyeong Heon Kim<sup>1</sup>, Seungbeom Noh<sup>1</sup>,  
Ashrafuzzaman Bulbul<sup>1</sup>, Ravi V Mural<sup>3</sup>, Aishwaryadev Banerjee<sup>1</sup>, James C. Schnable<sup>3</sup>, Mingyue Ji<sup>1</sup>,  
Carlos Mastrangelo<sup>1</sup>, Ling Zang<sup>2</sup>, and Hanseup Kim<sup>1</sup>*

<sup>1</sup>Electrical and Computer Engineering, University of Utah, Salt Lake City, UT 84112

<sup>2</sup>Materials Science and Engineering, University of Utah, Salt Lake City, UT 84112

<sup>3</sup>Department of Agronomy and Horticulture, University of Nebraska, Lincoln, NE 68588

### ABSTRACT

This paper reports the development of a high-sensitivity gas sensor and the demonstration of selectively detecting green leaf volatiles (GLV, here hexanal) released from damaged plant leaves. The developed sensor is a conductivity sensor that utilized a 5.2-nm gap as the key detection site between electrodes. The gap was coated with customized molecular probes toward binding to hexanal. The fabricated sensor demonstrated the detection of a GLV, hexanal, from the collected gas samples from damaged plant leaves, sorghum. Gas samples were collected into a tedlar bag from a glass jar containing damaged sorghum leaves. When exposed to hexanal concentrations from 77.7 to 5181.3 ppm, it produced output signal changes in resistance by 1.64~4.45 times. The sensor response time was measured as 41.6 min at a hexanal concentration of 77.7 ppm.

### KEYWORDS

green leaf volatiles (GLV), nano-gap, gas sensor

### INTRODUCTION

Green-leaf volatiles (GLV) detection has attracted much interest in the agriculture industry over the decades. GLVs are volatile organic compounds (VOCs) that are released from plants under stress, for example physical damage from pest attacks [1]. The type and the amount of GLVs released vary and could indicate the magnitude of damage and the source it was inflicted by.

Agriculture products have been damaged and lost significantly due to such as invasion of pests. Crop yield loss globally each year is estimated as about 35%, the economic impact of which can be reduced with early detection [2]. To mitigate the yield loss world wide pest control market was valued at 19.73 billion in 2019 [3]. Early detection of pest attacks on farms are necessary to mitigate the economic effect of damaged crops.

Current scouting and monitoring methods for pest detection have been limited by non-continuous monitoring, non in-situ monitoring for some and delayed data

processing due to sampling or post-processing requirement, as summarized in Table 1. Various methods have been utilized to detect pest attacks which either involve the deployment of sensors in the field or sample collection to be later analyzed by intricate lab equipment [4]. Optical methods involve utilizing an optical sensor in specific areas of the farms or pest traps to collect data in the form of images and in some cases involves a drone flying above the targeted area. However, they are limited in terms of continuity in monitoring due to excessive data storage and processing required from the continuous collection of images. They also often suffer resolution of the images to sufficiently distinguish pests out of the crops, and thus often require manual inspection by humans for visual confirmation [6]. This additional confirmation could cause delayed response. Thermographic methods utilize a thermal camera to map plant surface temperature which changes with stress level [7]. These cameras are often mounted on a unmanned aerial vehicles (UAV), which prevents continuous monitoring as well as requires significant amount of power. Fluorescence imaging involves imaging the chlorophyll content in plant leaves to determine whether they are in distress or not [8]. This fluorescence method, however, requires sampling processes from the field and post processing of the generated images, thus making continuous monitoring untenable. Chromatographic methods also involve sampling volatile organic compounds (VOCs) from farms, thus leading to time delay in detection, and require quite a complex systems like GC-MS [9]. Finally, acoustic sensors operate by detecting sound levels produced by insects above a predetermined threshold [5]. Acoustic sensors can perform continuous monitoring. They often requires post-data-processing to filter out noises in the backgrounds.

To enable continuous, non-delayed and in-situ monitoring, in this paper, we developed and utilize a gas sensor for the detection of a GLV. Specifically, we target to detect hexanal that has been reported to be released from a plant, sorghum, under stress in various concentrations. For example, hexanal emissions of 5-10 ppm have been reported [11].

*Table 1: Current plant damage detection methods*

	<i>This Work</i>	<i>Acoustic</i> <sup>5</sup>	<i>Optical</i> <sup>6</sup>	<i>Thermographic</i> <sup>7</sup>	<i>Fluorescence</i> <sup>8</sup>	<i>Chromatography</i> <sup>9</sup>
<b>Cont. Monitoring</b>	Yes	Yes	No	No	No	No
<b>Target</b>	GLV	Noise	Pest	Temperature	Radiation	GLV
<b>In-situ</b>	Yes	Yes	Yes	Yes	No	No
<b>Delayed Processing</b>	No	Yes	Yes	Yes	Yes	Yes

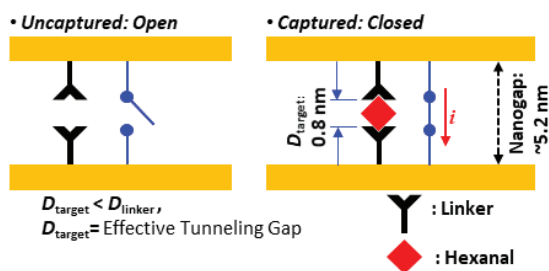


Figure 1: (Left) Disconnected molecular probes before target exposure and (Right) molecular probes bridging the nano-gap after exposure

Therefore, this paper reports the development of a high-sensitivity gas sensor and its first demonstration of the hexanal detection.

## HIGH SENSITIVITY GAS SENSOR

The detailed principles, fabrication, chemistry and preliminary results of the developed high-sensitivity gas sensor were reported in previous publications [12-15]. Thus, we will report only a brief summary.

### Operation principle

The developed gas sensor mainly consists of a nanometer sized gap (nano-gap) enclosed on two sides by large gold electrodes. The presence of the nano-gap ensures electrical separation between the two gold electrodes with only a negligible tunneling current flowing between them even when a biasing voltage is applied. When the sensor captures a specific target gas, based on matching gap sizes and affinity to the molecular probe, it increases the conductivity across the nanogap (Fig. 1). In this paper, the sensor is tailored to capture the target hexanal molecules.

### Synthesis of probe

To synthesize the molecular probe for coating with the required affinity, initially 0.31 g PTMM, 0.78 g ATP and 6g imidazole was taken in a round bottom flask. The mixture was heated under a nitrogen atmosphere at 100 °C for 6 hours. The reaction mixture was cooled to room temperature and dispersed in 400 mL ethanol/2M HCl (1:3). The mixture was stirred overnight. The resulting solid was collected by vacuum filtration and washed with distilled water until the neutral pH. The collected solid was dried in a vacuum at 60 °C to obtain the probes.

The resulting probe has a highly  $\pi$ -conjugated structure and is conductive in nature. It possessed a core structure that allows a high flexibility for modifications of the side binding group, but without altering the electrical property (like resistance) of the backbone structure. The probe consists two thiol (-SH) functional groups on both sides. One side of the linker was bonded to the gold electrode via Au-S covalent bond, while the other side remained available for the bonding to the target hexanal molecule.

### Microfabrication of the sensor structure

The required gap structure was constructed by vertically stacking electrodes, which were sputter-

deposited, with the nano-gap enclosed in between [16]. An average gap size of 5.2 nm gap was selected to match the combined length of the linker (2~2.5 nm) and the hexanal molecule (0.5~0.7 nm). The 5.2 nm gap was accurately defined by atomic layer deposition of silicon dioxide (SiO<sub>2</sub>) and a thin amorphous silicon layers. The nano-gap was formed by removing both silicon dioxide (SiO<sub>2</sub>) and silicon layers via reactive ion etching (RIE). Effective nano-gap areas of the nano-gap was estimated to be ~125  $\mu\text{m}^2$ .

### Sensor coating with molecular probes

The fabricated nano-gap structure was submerged into a solution containing the probes and DMF solvent for 36 hours to allow the self-assembled monolayer (SAM) to form on the gold surface. After 36 hours of coating the sensors were taken out and cleaned with DMF/Acetone. Finally, the sensors were dried in a vacuum chamber and stored in vacuum until testing.

### Gas sample collection

Gas samples were collected into a tedlar bag (in Nebraska) by flowing gases from a jar with damaged leaves through a pump into the bag, as shown in Fig. 2. For the sampling, the gas flow was maintained by utilizing an ACTI-VOC low flow pump (Markes) at a flow rate of 25 ml/min for 20 mins. Three samples were collected in total; 1st being gas collected from undamaged leaves as the control, 2nd being gas collected from leaves in green house, and 3rd being gas collected from leaves in field.

## EXPERIMENTAL PROCEDURE

### Confirming Hexanal as a plant signature GLV

To determine the presence of hexanal the collected air samples were run through the GC-MS with the help of a sorbent tube. The resultant spectrum from the GC-MS were then compared with a known standard library from NIST to identify the hexanal peak. An additional control sample not containing hexanal was added to validate the testing results.

### Detection of Hexanal with the fabricated sensor

Gas samples were then used to test the sensor to determine its response to the hexanal. Sensors were placed in the testing chamber of which the inlet was connected to a tedlar bag containing gas samples collected from damaged leaves (Fig. 2).



Figure 2: Gas Sample collected from damaged leaves

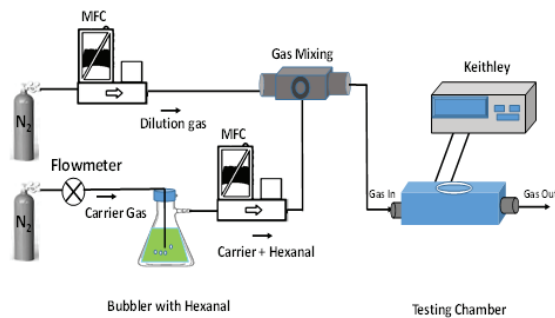


Figure 3: Experimental setup for commercial hexanal testing

The fabricated sensor was tested with all three samples collected in a 1 liter tedlar bag. Tedlar bags were connected to a MFC leading to the inlet of the testing chamber. During testing the valve in the tedlar bag was opened, and a flow of the gas sample was allowed. During the flow, the change in resistance of the sensor was observed.

### Estimation of hexanal concentration in samples

The fabricated sensors were then tested with known concentrations of commercially obtained hexanal to set up a calibration curve and determine the exact concentration of hexanal present in the collected gas samples. Figure 3 shows the experimental testing set-up to confirm the responses of the fabricated sensor to various concentrations of commercial hexanal (MilliporeSigma). The fabricated sensor was placed in a micro probe station (MPS) testing chamber (Nextron). The inlet of the testing chamber was connected to a gas mixing chamber where dilution of pure hexanal vapors occurred. Concentrations of hexanal were controlled from 77.74 ppm to 5181.34 ppm.

## RESULTS

### Confirmation of hexanal as a plant signature GLV

The resultant GC spectrum showed a transient peak for hexanal at 3.716 min, and the peak was further analyzed via the mass spectrometer (MS) to show mass-to-charge ratios, as shown in Fig. 4. The mass spectrum (MS) of each peak was compared to the corresponding spectrum in the

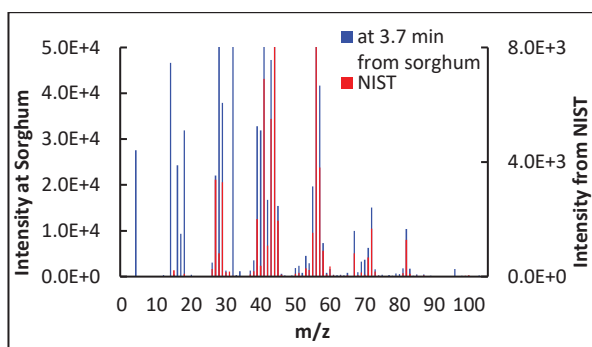


Figure 4: Confirmation of hexanal from sorghum leaves by utilizing mass-spectrometry. The measurement was compared to a standard library from the National Institute of Standards and Technology (NIST) in US.

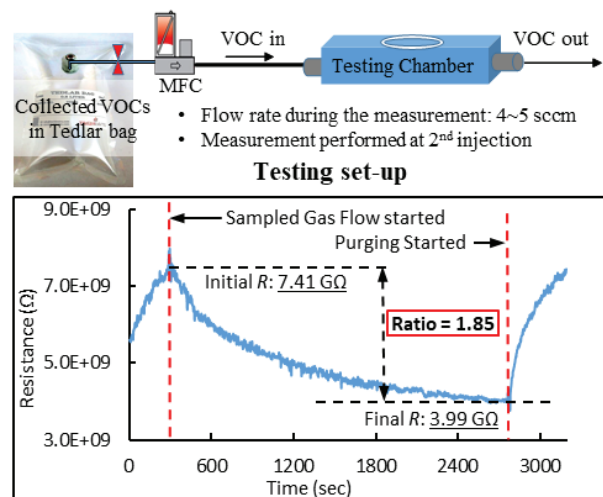


Figure 5: (Top) Experimental setup for Tedlar bag (Bottom) Response ratio of 1.85 due to exposure from collected gas sample

National Institute of Standards and Technology (NIST) standards. The obtained GC-MS spectrum from the peak at 3.716 min in gas chromatogram, overall matched to the NIST hexanal standard, confirming that hexanal was released as a dominant GLV by damaged sorghum leaves. Such a peak was confirmed in the damaged leaf gas samples and not in undamaged leaf sample (control), as expected.

### Detection of hexanal with the fabricated sensor

Upon exposure of the gas sample, the sensor output in resistance started decreasing by 1.15 times for sample 1 (control); by 1.82 times for sample 2 and by 1.85 times for sample 3 indicating the presence of hexanal in samples 2 and 3, as shown in Fig. 6. Figure 5 is the response of the sensor output when exposed to the sample 3. During this testing, flow rates of the gas samples were maintained

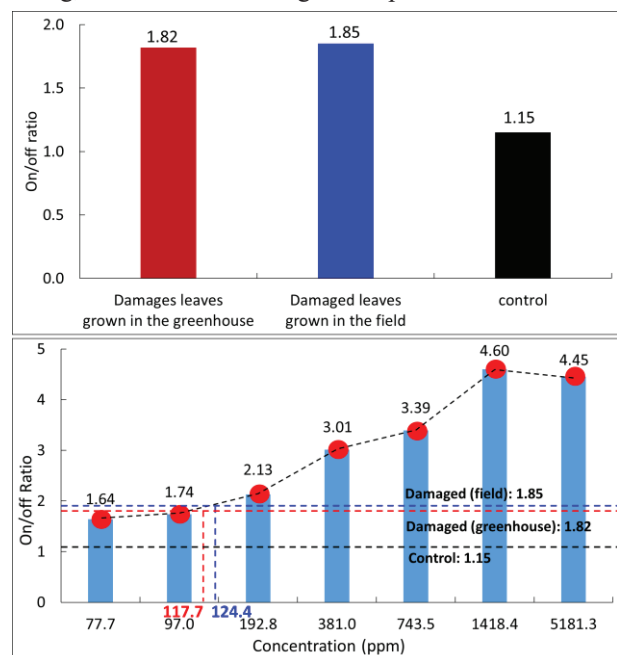


Figure 6: (Top) Sensor response to collected gas samples (Bottom) Sensor response at various concentrations of commercial hexanal

between 4~5 sccm. Note that the output response was fully recovered once the hexanal gas is purged out of the test chamber.

### Estimation of hexanal concentration in samples

Experimental results showed that the gas sensor responses, when exposed to concentrations ranging from 77.7 ppm to 5181.34 ppm, resulted in output signal changes in resistance from 1.64 times to 4.45. Figure 6 (Bottom) shows that the response ratios were 1.64 times for 77.74 ppm, 1.74 for 97.04 ppm, 2.13 for 192.8 ppm, 3.01 for 380.95 ppm, 3.39 for 743.49 ppm, 4.6 for 1,418.44 ppm and 4.45 for 5,181.34 ppm of hexanal. The trend was mostly linear at lower concentrations (77.4 to 1418.44 ppm) with a fitting curve equation of  $y=0.0045x + 1.29$ , which served as the calibration curve.

Based on the calibration curve, the sensor output under the exposure to hexanal in samples was estimated as 117.7 ppm in damaged leaves in greenhouse sample and 124.4 ppm in damaged leaves in field sample. The measured sensor output signals in resistance ratios were 1.82 and 1.85 respectively.

### CONCLUSION

This paper has reports the development and the demonstration of a high-sensitivity gas sensor that is capable of real time detection of hexanal released from a plant leaves, sorghum. The sensor responded with a ratio of 1.85 when tested with gas samples collected from damaged leaves, in comparison to 1.15 for undamaged leaves, and thus confirmed the release of hexanal from leaves under stress and the detection capability of the developed sensor. The sensor response, by comparing with a calibrated curve data, was confirmed for its detection of hexanal in 117.7 ppm (damaged leaves\_greenhouse) and 124.4 ppm (damaged leaves\_field) directly from a jar that contained damaged leaves of a plant, sorghum.

### ACKNOWLEDGEMENT

This research work was generously supported by the cooperative agreement of DE-AR0001064 of the ARPAE OPEN 2018 program (Program Manager: Dr. David Babson). Microfabrication was performed at the Utah Nanofabrication Facility at the University of Utah.

### REFERENCES

- [1] Martinelli, F., Scalenghe, R., Davino, S. et al. Advanced methods of plant disease detection. A review. *Agron. Sustain. Dev.* 35, 1–25 (2015).
- [2] "Studies in Agricultural Economics No.113" Research Institute of Agricultural Economics Committee on Agricultural Economics, Hungarian Academy of Sciences, 2011.
- [3] "Pest Control Market Size Worth USD 31.94 Billion by 2027; Rising Adoption of Pest Control Software will Add Impetus to Market, Says Fortune Business Insight" June 05, 2020.
- [4] Adedeji, Akinbode et. al "Non-Destructive Technologies for Detecting Insect Infestation in Fruits and Vegetables under Postharvest Conditions: A

Critical Review" (2020).

- [5] Prince P, Hill A, Piña Covarrubias E, Doncaster P, Snaddon JL, Rogers A. Deploying Acoustic Detection Algorithms on Low-Cost, Open-Source Acoustic Sensors for Environmental Monitoring. *Sensors*. 2019; 19(3):553.
- [6] López O, Rach MM, Migallon H, Malumbres MP, Bonastre A, Serrano JJ. Monitoring Pest Insect Traps by Means of Low-Power Image Sensor Technologies. *Sensors*. 2012; 12(11):15801-15819.
- [7] Messina G, Modica G. Applications of UAV Thermal Imagery in Precision Agriculture: State of the Art and Future Research Outlook. *Remote Sensing*. 2020; 12(9):1491.
- [8] Mei, L., Guan, Z.G., Zhou, H.J. et al. Agricultural pest monitoring using fluorescence lidar techniques. *Appl. Phys. B* 106, 733–740 (2012).
- [9] Martinelli, F., Scalenghe, R., Davino, S. et al. Advanced methods of plant disease detection. A review. *Agron. Sustain. Dev.* 35, 1–25 (2015).
- [10] Scala A, Allmann S, Mirabella R, Haring MA, Schuurink RC. Green leaf volatiles: a plant's multifunctional weapon against herbivores and pathogens. *Int J Mol Sci*. 2013;14(9):17781-17811. Published 2013 Aug 30.
- [11] L.M. Seitz and D. B. Sauer "Volatile Compounds and Odors in Grain Sorghum Infested with Common Storage Insects", *Cereal Chem.* 73(6):744-750.
- [12] S.H. Khan et al. "Ultra-low-power chemical sensor node". In Proceedings of the GOMAC Tech. 2018, Miami, FL, USA, 12–15 March 2018.
- [13] S.H. Khan, et. al "Molecular Length Based Target Identification using a Nano-Gap Sensor," 2019 IEEE 32nd International Conference on *Micro Electro Mechanical Systems (MEMS)*, Seoul, Korea (South), 2019, pp. 460-463.
- [14] S. H. Khan, et. al, "2019 IEEE 32nd International Conference on *Micro Electro Mechanical Systems (MEMS)*, Seoul, Korea (South), 2019, pp. 137-140.
- [15] "Unpublished Reference"
- [16] Banerjee, A et. al "Batch Fabricated  $\alpha$ -Si Assisted Nanogap Tunneling," *Nanomaterials* 2019, 9, 727.

### CONTACT

\*H. Kim, tel: +1-801-5879497; hanseup.kim@utah.edu